AUTO TAPER TENSION PROFILE MAKER IN A CONVERTING MACHINE

by

C.W. Lee,[1] J.W. Lee,[1] K.H. Shin,[1] and S.O. Kwon[2]
[1]KonKuk University
[2]Sung-An Machinery
KOREA

ABSTRACT

Winding is an integral operation in almost every web handling processes. Center-wounding are suitable and a general scheme in winding systems. However, the internal stresses within center-wound rolls can cause damage such as buckling, spoking, cinching, etc. Wound roll quality and performance are known to be related to distribution of in-roll stresses. It is therefore necessary to analyze the relationship between taper tension in winding section and internal stress distribution within center-wound roll to prevent the potential winding failure (starring, buckling, telescoping, etc.).

In this study, a new taper tension control method for producing high quality wound roll was developed. The new method was induced from analyzing the winding mechanism by using the stress model in center-wound rolls, nip induced tension model, taper tension profile-telescoping relationship, and taper tension type-internal stresses relationship, etc. Auto taper tension profile making method for avoiding the damage (telescoping, buckling, cinching, etc.) is presented. The experimental results show that the proposed method is very useful.

NOMENCLATURE

a = core radius, m
B = arbitrary constant
EI = bending stiffness, Nm^2
L = length of span, m
r = build-up ratio, dimensionless
R = outer roll radius ratio, dimensionless
s = elastic compliance, m^2/N
T = operating tension, N/m
α = hybrid factor, dimensionless
ν = poisson ratio, dimensionless
σ = stress

Scripts

0 = initial

* = residual

rr = radial

INTRODUCTION

Web handling is a manufacturing process which pervades almost every manufacturing industry. Winding is an integral operation in almost web handling systems. Centre wound roll form is the most efficient and convenient storage format for high speed winding process. However, the internal stresses within centre wound rolls can cause damage such as buckling, spoking, cinching, etc. It is therefore desirable to wind just enough stress into a wound roll that a stable package is wound without inordinate or insufficient stress.

Early work [4] provided a general solution for a linear elastic roll material while using a nonlinear constitutive relation to find the radial and hoop stresses for successive wraps. Altmann solved a second order differential equation for the linear elastic material in a centre wound roll [l]. Yagoda established the core compliance as an inner boundary condition on centre wound rolls [5]. Hakiel incorporated nonlinear material properties into the basic mechanics and numerical solutions of wound roll stresses [3]. Good compared results from Hakiel's model with interlayer pressure measurements obtained using pull tabs [2]. They noted that the model typically predicted stresses that were twice as large as their measured values. However, they were able to bring predicted and measured values into better agreement by modifying the outer hoop-stress boundary condition to relax relative to the out-layer tensile stresses by their model of "wound on tension" loss. Burns derived a strain-based formula for stresses in profiled centre wound rolls by using residual stress model [1]. They noted that radial stress within wound roll is closely related to the variation of effective radial stress.

After reviewing the literature, it is clear that a momentous factor for making high quality wound roll is the taper tension profile in winding processes. In this paper, an auto taper tension profile making method for avoiding the damage (telescoping, buckling, cinching, etc.) is presented. The experimental results show that the proposed method is very useful.

TAPER TENSION MODEL IN WINDING PROCESS

Figure 1 is a schematic geometry of the tension T acting on the web and roll. In the Figure 1, a is core radius, R is current radius of roll, M is torque, and σ_w is a taper tension profile.

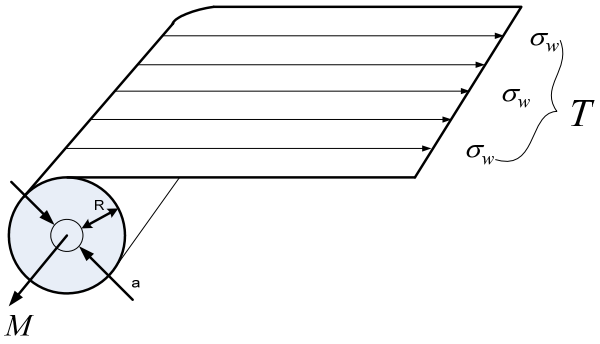

Figure 1 – Schematic of centre wound roll

In a general way, a linear and hyperbolic taper tension profile is applied to winding process [2][3]. The linear and hyperbolic taper tension profile can be represented as the following equation {1} and {2}. σ_0 is initial web stress, *taper* is the decrement of taper tension and r is dimensionless roll radius ratio, i.e., the radius divide by the core radius.

$$\sigma_w(r) = \sigma_0 \left[1 - \left(\frac{taper}{100} \right) \frac{(r-1)}{(R-1)} \right] \quad \{1\}$$

$$\sigma_w(r) = \sigma_0 \left[1 - \left(\frac{taper}{100} \right) \left(\frac{r-1}{r} \right) \right] \quad \{2\}$$

Figure 2 shows the taper tension plotted as a taper tension ratio, i.e., $\sigma_w(r) / \sigma_0$, for the two profiles. The hyperbolic taper tension variation seen in wound roll is larger at the core and smaller on the outer layer. But the linear taper tension variation is constant.

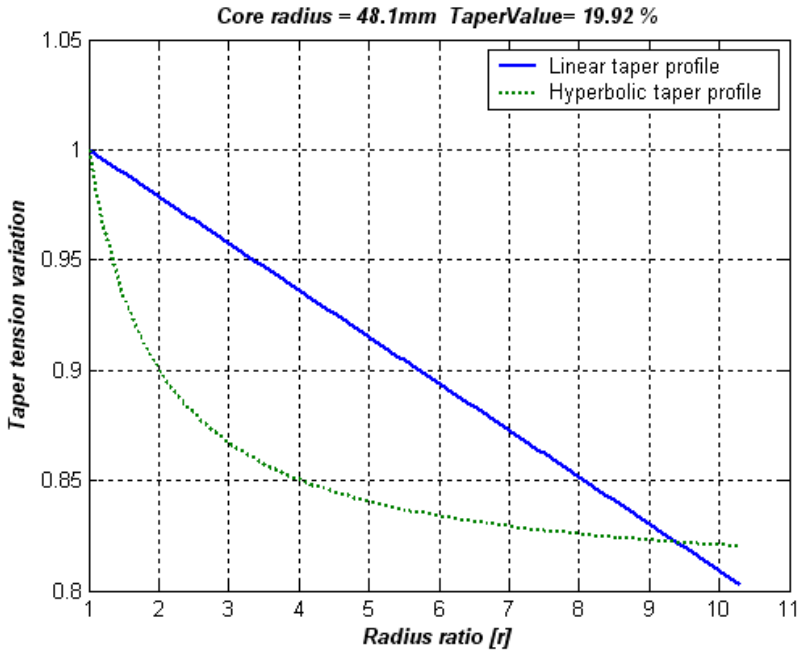

Figure 2 – Linear and hyperbolic taper tension profile

RADIAL STRESS MODEL IN WOUND ROLL

The boundary condition is that the outside of the roll is stress free. Thus stress for the radial direction within wound roll is given in equation {3} [1].

$$\sigma_{rr} = \frac{1}{r}\left\{\left[B\left(r^{\beta} - \frac{R^{2\beta}}{r^{\beta}}\right)\right] + \frac{1}{2\beta}\left[r^{-\beta}\int_{r}^{R} t^{\beta}\sigma^{*}(t)dt - r^{\beta}\int_{r}^{R} t^{-\beta}\sigma^{*}(t)dt\right]\right\} \qquad \{3\}$$

where

$$B = \frac{2\beta\sigma_0 E_c s_{22} - \left\{\left[E_c\left(s_{12} - \beta s_{22}\right) - 1\right]\int_{1}^{R} t^{\beta}\sigma^{*}(t)dt\right\} - \left\{\left[E_c\left(s_{12} - \beta s_{22}\right) - 1\right]\int_{1}^{R} t^{-\beta}\sigma^{*}(t)dt\right\}}{2\beta\left[\left(s_{12}E_c - 1\right)\left(1 - R^{2\beta}\right) + \beta E_c s_{22}\left(1 + R^{2\beta}\right)\right]} \qquad \{4\}$$

and

$$\beta^2 = \frac{s_{11}s_{33} - s_{13}^2}{s_{22}s_{33} - s_{23}^2} \qquad \{5\}$$

In equation {3} and {4}, E_c is the hub core stiffness and s_{11}, s_{13}, s_{22}, s_{23}, s_{33} is the roll's elastic compliances. Substituting the ERS into equation {3} results in equation {6} which means the radial stress for the linear taper tension profile. The radial stresses for

the hyperbolic taper tension profile can be represented as following equation {7} from equation {2}.

$$\sigma_{rr} = \frac{1}{r}\left\{\left[B\left(r^{\beta} - \frac{R^{2\beta}}{r^{\beta}}\right)\right] + \left(\frac{1}{2\beta}\right)\left(\frac{\sigma_0}{1-\nu}\right)\left[\left(\frac{R^{\beta+1} - r^{\beta+1}}{\beta+1}\right)r^{-\beta} + \left(\frac{R^{1-\beta} - r^{1-\beta}}{\beta-1}\right)r^{\beta}\right]\left\{\left(\frac{2+\nu}{1+\nu}\right)\left(\frac{1}{R-1}\right)\left(\frac{taper}{100}\right) - \left[1 + \left(\frac{1}{R-1}\right)\left(\frac{taper}{100}\right)\right]\right\}\right\} \quad \{6\}$$

$$\sigma_{rr} = \frac{1}{r}\left\{\left[B\left(r^{\beta} - \frac{R^{2\beta}}{r^{\beta}}\right)\right] + \frac{\sigma_0}{2\beta}\left\{\left(\frac{1}{1-\nu}\right)\left(1 - \frac{taper}{100}\right)\left[\left(\frac{R^{\beta+1} - r^{\beta+1}}{\beta+1}\right)r^{-\beta} - \left(\frac{R^{1-\beta} - r^{1-\beta}}{1-\beta}\right)r^{\beta}\right] + \nu\left(\frac{1}{1-\nu^2}\right)\left(\frac{taper}{100}\right)\left(\frac{\left(\frac{R}{r}\right)^{\beta} - \left(\frac{r}{R}\right)^{\beta} - 2}{\beta}\right)\right\}\right\} \quad \{7\}$$

Figure 3 shows the radial stresses plotted as a $-\sigma_{rr} / \sigma_0$ for the two taper tension profiles. On the whole, the radial stress distribution for the hyperbolic profile has equipollence more than for the linear taper profile.

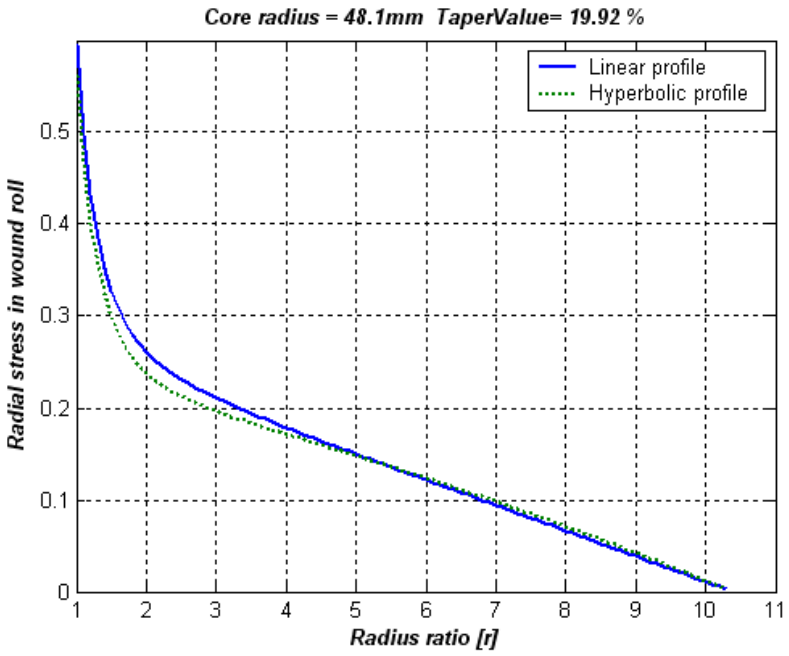

Figure 3 – Radial stress for two taper tension profiles

HYBRID TAPER TENSION CONTROL

Correlations between ERS and radial stress within wound roll

Figure 4 shows the variation of the ERS value for two taper tension profiles. In Figure 3 and 4, the close correlation between ERS and radial stress can be found. As derivative of the ERS value is low, as distribution of the radial stress is small and equable.

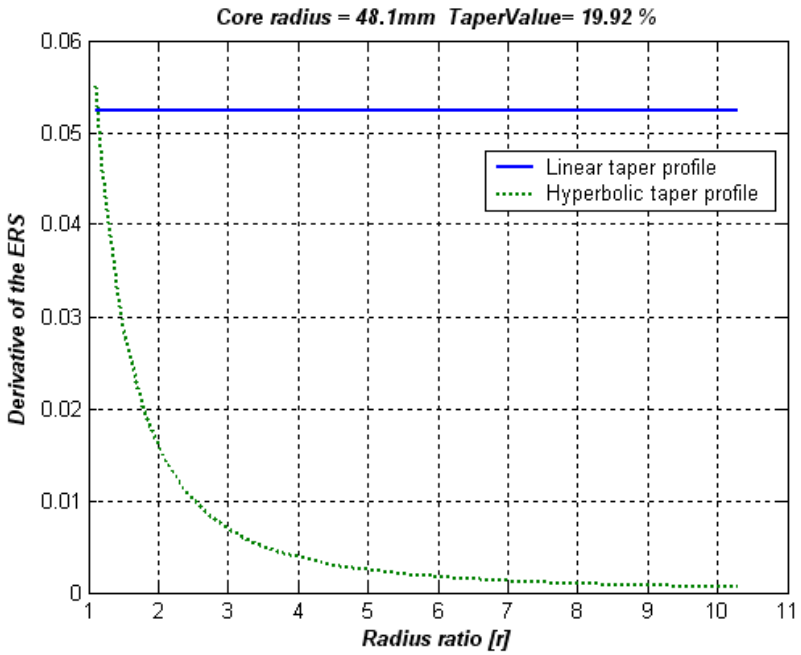

Figure 4 – Derivative of the effective residual stress

In the view of the above results, it is found that hyperbolic taper tension profile prevents intensive increment of radial stress and promotes uniform radial stress distribution.

Relationships between taper tension profile and telescoping in winding processes

Camber can be expressed as the radius of the curvature in the un-tensioned condition and lying on a flat surface. Assuming linear stress distribution in the cambered web as shown in Figure 7, the induced moment can be found in equation {8}.

$$M = r \times F = \left(\frac{W}{6}\right)\left(T_{\max} - T_{\min}\right) = \frac{\left(T_{\max} - T_{\min}\right)}{6} W \qquad \{8\}$$

From beam theory, curvature is

$$\rho = \frac{EI}{M} \qquad \{9\}$$

Substituting M of equation {8} for equation {9} leads the curvature model as shown in equation {10}

$$\rho = \frac{6EI}{(T_{\max} - T_{\min})W} \qquad \{10\}$$

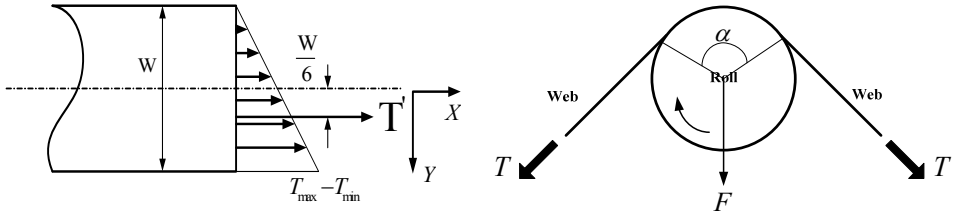

Figure 5 – Uneven tension distribution in CMD and wrap angle

Figure 6 identifies the elastic behavior of the web under general movement of roller.

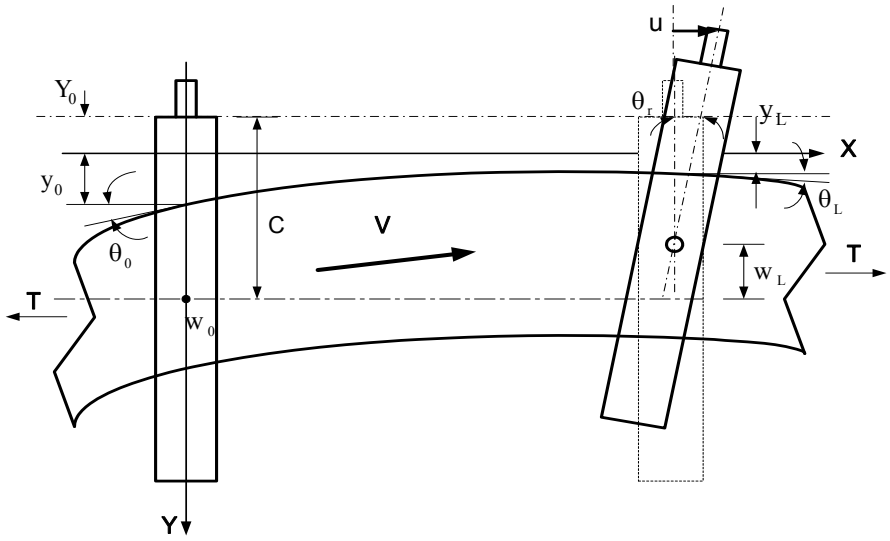

Figure 6 – Boundary condition in a span

In Figure 6, lateral deflection at a downstream roller is determined such as equation {11} [7] [8].

$$y_L = \frac{2 - 2\cosh(KL) + \sinh(KL)KL}{\rho K^2 \left(\cosh(KL) - 1\right)} \qquad \{11\}$$

The y_L of equation {11} is equal to telescoping error in winding process, because downstream roller is a wound roll. Therefore, through the correlation between lateral

deflection and tension distribution, the mathematical model for telescoping can be defined as shown in equation {12}.

$$y_{telescoping} = \frac{2 - 2\cosh(KL) + \sinh(KL) \cdot KL}{\left[\frac{12EI}{(F_{\max} - F_{\min})W} \sin\left(\frac{\alpha}{2}\right)\right] K^2 \left(\cosh(KL) - 1\right)} \quad \{12\}$$

where, is stiffness coefficient, is force given by web tension and K is stiffness coefficient, F is force given by web tension and α is wrap angle.

Under the condition of same uneven tension distribution in CMD as shown in Figure 5, computer simulations to analysis the relationships between taper tension type and telescoping are carried out. It is found that taper tension type can affect the telescoping magnitude, as can be seen in Figure 7, because they have quite different variation according to the winding radius.

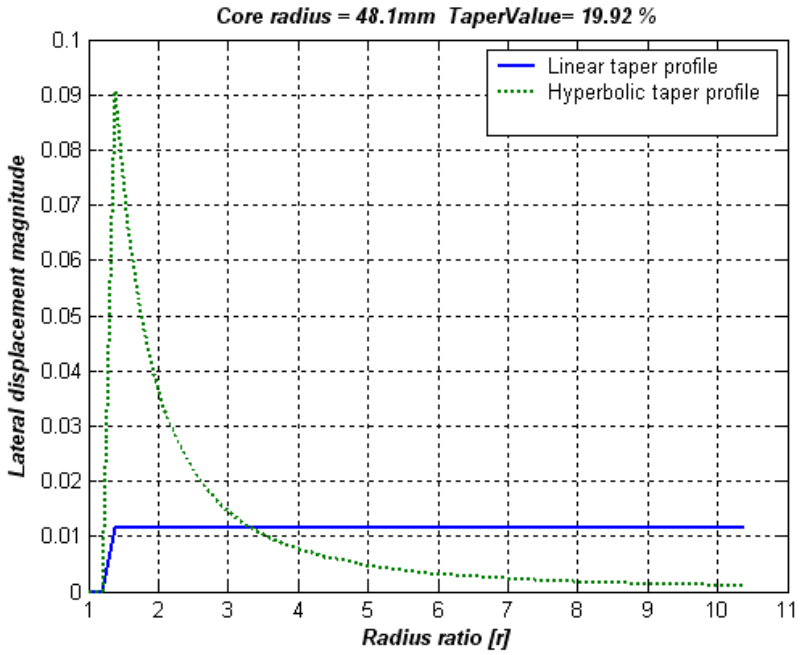

Figure 7 – Telescoping in winding roll

Hybrid taper tension profile in winding processes

Figure 4 shows that the derivative (rate of the variation) of ERS according to wound roll radius could be obtained lower by hyperbolic taper tension profile than the linear taper tension profile. Small derivative of the ERS makes the radial stress distribution lower and even also as shown in Figure 9 and Figure 10.

These results say that the hyperbolic tension profile is more advantageous in view of radial stress distribution. But from Figure 7, the possibility and magnitude of telescope of wound roll near the outside of core are much higher when the taper tension profile is applied during the winding process.

The linear taper tension profile is more advantageous to prevent the telescope of the wound roll in the beginning of winding process. But it could make the radial stress distribution higher as shown in Figure 10 and Figure 11. Hybrid taper tension profile could be designed to take advantages of each linear and hyperbolic taper tension profile by combining both algorithms.

Equation {12} shows the mathematical model of the hybrid taper tension profile. The models of ERS and radial stress distribution of wound roll using the hybrid taper tension profile are equation {13} and {14}.

$$\sigma_w(r) = \sigma_0 \left[1 - \left(\frac{taper}{100} \right) \frac{(r-1)}{\{r + \alpha \cdot (R - r - 1)\}} \right] \qquad \{13\}$$

$$\sigma^*(r) = \left[\frac{\sigma_0}{1-\nu^2} \right] \left\{ (1+\nu) - \left(\frac{taper}{100} \right) \left(\frac{\left(r^2 + \nu(r^2 - r)\right) + \alpha \cdot \left[(R-r-1)\left[(1+\nu)(r-1) + r \right] + r(r-1) \right]}{\left[r + \alpha \cdot (R - r - 1) \right]^2} \right) \right\} \qquad \{14\}$$

$$\sigma_{rr} = \frac{1}{r} \left\{ \left[B\left(r^\beta - \frac{R^{2\beta}}{r^\beta} \right) \right] + \left(\frac{1}{2\beta} \right) \left(\frac{\sigma_0}{1-\nu^2} \right) \left\{ \begin{array}{l} \left[\left(\frac{1+\nu}{1+\beta} \right) \left(\frac{R^{1+\beta}}{r^\beta} - r \right) - \left(\frac{taper}{100} \right) r^{-\beta} \int_r^R t^\beta \left(\frac{\left(t^2 + \nu(t^2 - t)\right) + \alpha \cdot \left[(R-t-1)\left[(1+\nu)(t-1) + t \right] + t(t-1) \right]}{\left[t + \alpha \cdot (R-t-1) \right]^2} \right) dt \right] \\ - \left[\left(\frac{1+\nu}{1-\beta} \right) \left(\frac{r^\beta}{R^{1-\beta}} - r \right) - \left(\frac{taper}{100} \right) r^\beta \int_r^R t^{-\beta} \left(\frac{\left(t^2 + \nu(t^2 - t)\right) + \alpha \cdot \left[(R-t-1)\left[(1+\nu)(t-1) + t \right] + t(t-1) \right]}{\left[t + \alpha \cdot (R-t-1) \right]^2} \right) dt \right] \end{array} \right\} \right\} \qquad \{15\}$$

Weight factor α in equation {12} determines the contribution to both of linear and hyperbolic profile in designing a new hybrid taper tension profile. The value 1 and 0 of α means linear and hyperbolic taper tension profile respectively as shown in Figure 8.

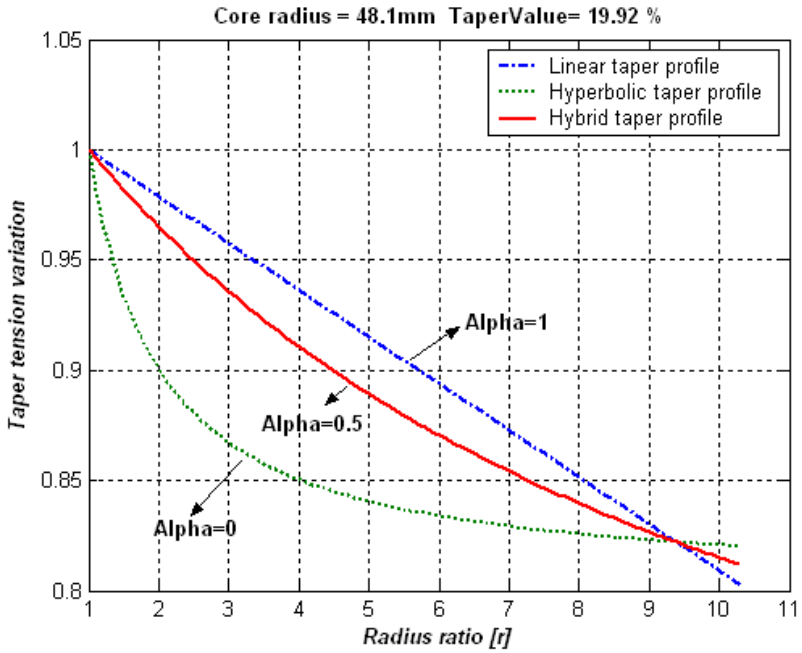

Figure 8 – Hybrid taper tension profile

Figures 9 ~ 11 show simulation results of the ERS, radial stress distribution, and induced telescope of wound roll when the hybrid taper tension profile is applied to winding process. From these simulation results, it was found that applying the hybrid taper tension profile during winding process can reduce the magnitude of radial stress distribution and telescope in wound rolls within the satisfying boundary.

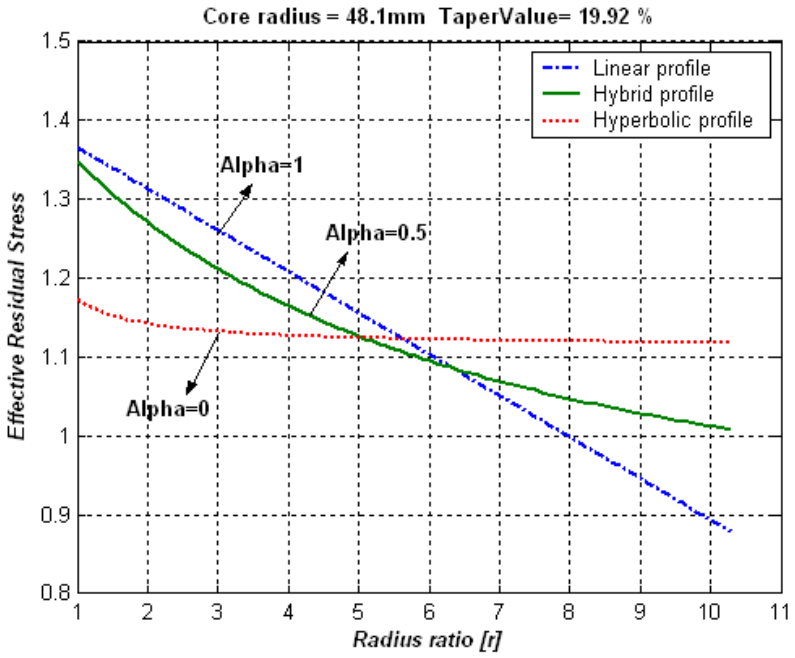

Figure 9 – ERS for three taper types

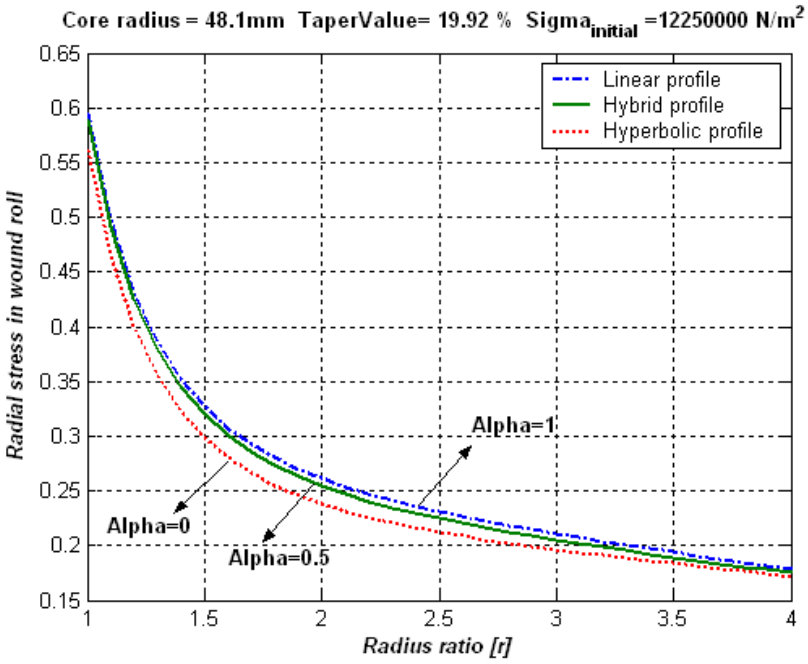

Figure 10 – Radial stresses for three taper types

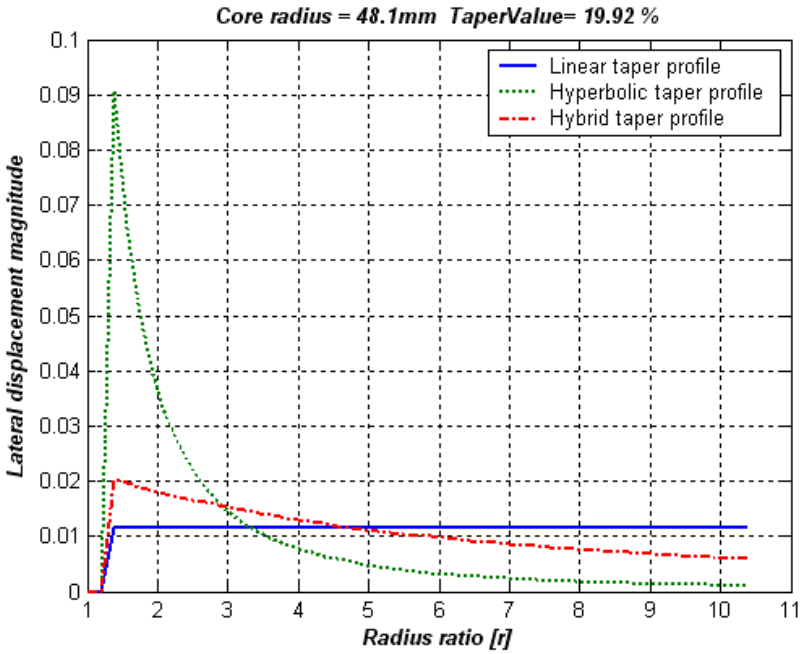

Figure 11 – Induced telescoping for three taper types in rewinding roll

HEAVISIDE TAPER TENSION CONTROL

In Figure 11, Lateral displacement is very different according to the types of taper tension profile. In the beginning of rewinding(r<2), the telescoping problem is so serious. After that(r>2), the radial stress distribution is so important (Figure 10, Figure 11). In order to minimize telescoping and to optimize radial stress distribution, a heaviside taper tension profile is proposed such as equation {16}.

$$\sigma_w(r) = \sigma_0 \left[1 - \left(\frac{taper}{100} \right) \frac{(r-1)}{\left\{ r + (R-r-1) \cdot \left[1 - \Phi(r-\tau) \right] \right\}} \right]$$

$$\Phi(r-\tau) = \begin{cases} 0 & r < \tau \\ 1 & r \geq \tau \end{cases} \qquad \{16\}$$

where, Φ means heaviside function. In equation {16}, the type of taper tension profile is changed according to increasing build up ratio(r). Namely, the type of taper tension profile can be changed by Φ according to increasing build up ratio(r) as shown in Figure 12.

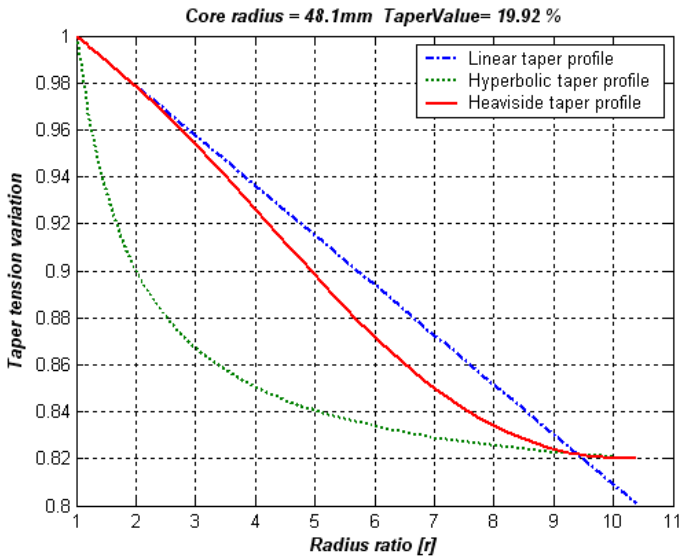

Figure 12 – Heaviside taper tension profile

EXPERIMENTAL VERIFICATION

The roll-to-roll system which was used for the experiment are composed of unwinding, in-feeding, printing, out-feeding and, winding sections as shown in Figure 13. Table.1 shows the experimental conditions.

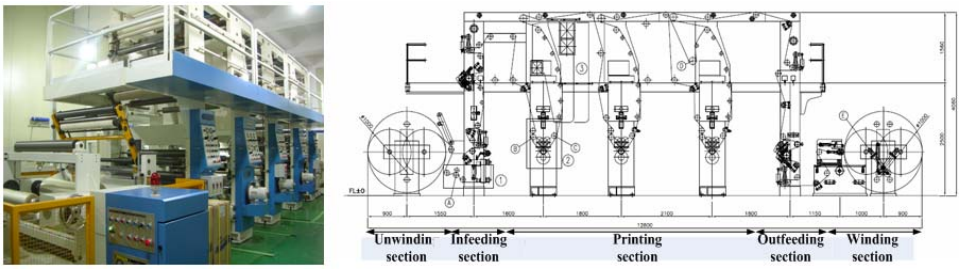

Figure 13 – A roll-to-roll system

Thickness of OPP (mm)	0.02
Width of OPP (mm)	1010
Poisson's ratio of OPP	0.3
Hybrid factor(α)	1(linear), 0(hyperbolic), 0.5(hybrid)
Young's modulus (MPa)	1180

Table 1 - Experiment conditions

There are four types of taper tension profiles as shown in Figure 14. From the experimental results, it is confirmed that the taper tension in winding system follows the reference tension profile. The type of taper tension profile is determined by hybrid factor (α) as shown in equation {12} and is determined by heavies function (Φ) as shown in equation {16}.

Figure 15 shows experimental results of the radial stress distribution. In Figure 15 and Figure 16, the correlation between taper tension and radial stress is confirmed. Finally, the radial stress for linear taper tension (Figure 15 (a)) is larger than other taper tension profiles. In the view of this result, the hyperbolic taper tension is more effective for preventing starring problem. But the hyperbolic taper tension may cause a telescoping as shown in Figure 16 (b). Figure 16 shows measured lateral error by EPS (Edge Position Sensor).

Namely, it is needed to find out an optimal taper tension profile for preventing starring and minimizing telescoping. Finally, a heaviside taper tension profile are proposed. The experiment results show that the performance of the proposed a heaviside tension profiles is very effective for minimizing the telescoping and for preventing the starring problem as shown in Figure 15 and Figure 16.

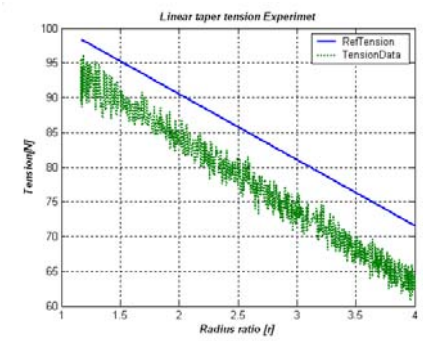

(a) Linear taper tension profile

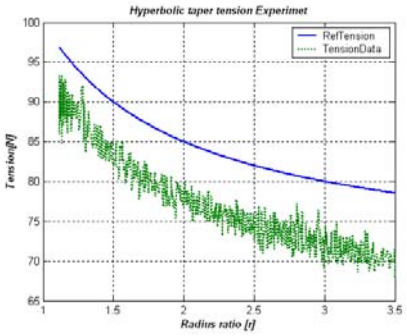

(b) Hyperbolic taper tension profile

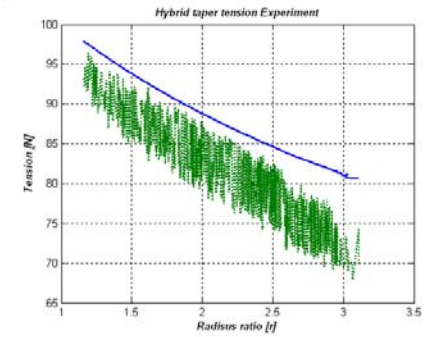

(c) Hybrid taper tension profile

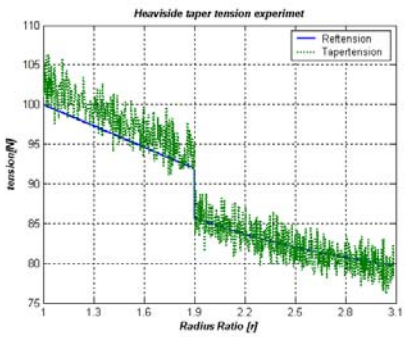

(d) Heaviside taper tension profile

Figure 14 – Taper tension profiles (experiments)

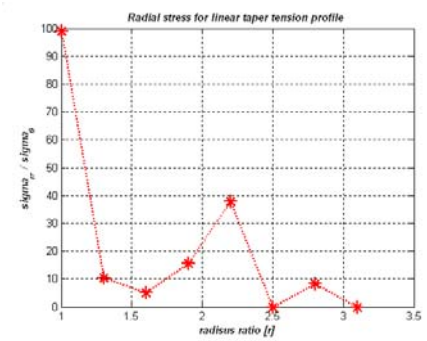

(a) Radial stress for linear profile

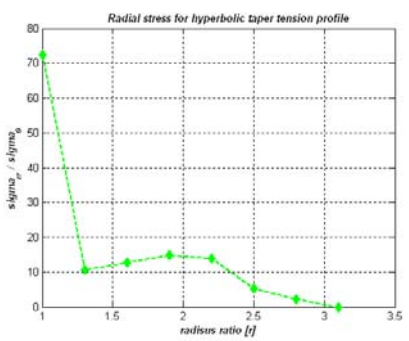

(b) Radial stress for hyperbolic profile

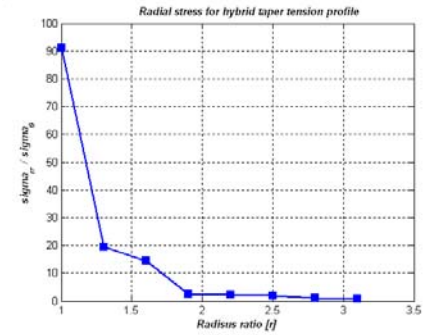

(c) Radial stress for hybrid profile

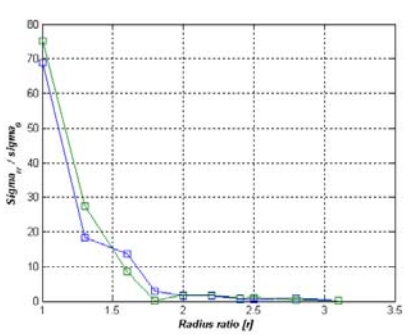

(d) Radial stress for heaviside profile

Figure 15 – Radial stress distribution for each types of taper tension

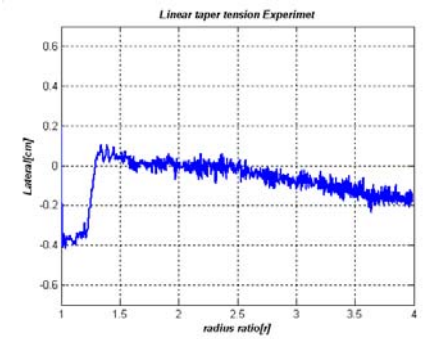

(a) Lateral error for linear profile

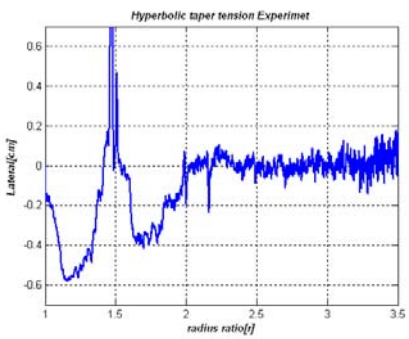

(b) Lateral error for hyperbolic profile

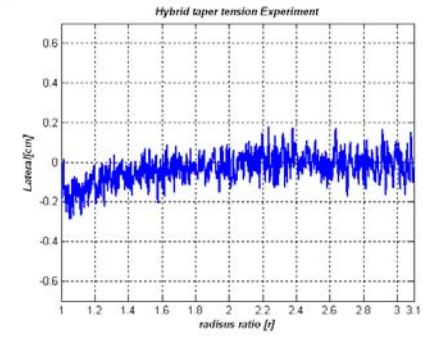

(c) Lateral error for hybrid profile

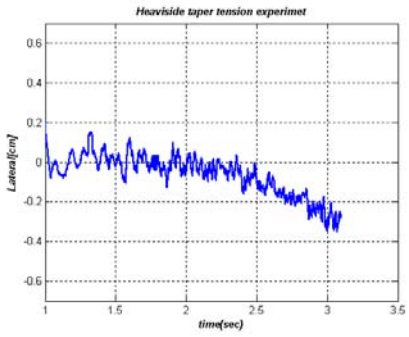

(d) Lateral error for heaviside profile

Figure 16 – Lateral error for each types of taper tension

CONCLUSION

The effect of taper tension profile during winding process on the radial stress distribution and telescoping phenomena was analyzed. In this study, a new hybrid taper tension profile and a heaviside taper tension profile were designed to prevent starring and minimize telescoping in winding system. And its performance was verified by computer simulations and experiments.

REFERENCES

1. Burns, S. J., Meehan, R. Richard, and Lambropoulos, J. C., "Strain-based Formulas for Stresses in Profiled Center-Wound Rolls," Tappi Journal, Vol. 82, 1999, pp. 159-167.
2. Good, J. K., Pfeiffer, J.D., and Giachetto, R.M., "Losses in Wound-On-Tension in the Center Winding of Wound Rolls," Proceeding of the Web Handling Symposium. ASME Applied Mechanics Division, AMD-Vol. 149, 1992, pp. 1-12
3. Hakiel, Z., "Nonlinear model for wound roll stresses," Tappi Journal, Vol. 70, 1987, pp. 113-117

4. Altmann, Heinz C., “Formulas for Computing the Stresses in Center-Wound Rolls,” Tappi Journal, Vol. 51, 1968, pp. 176-179.
5. Yagoda, H. P., “Resolution of a Core Problem in Wound Rolls,” Journal of Applied Mechanics, Vol. 47, 1980, pp.847-854.
6. Shelton, J., “Lateral Dynamics of a Moving Web,” Ph. D. Dissertation, Oklahoma State Univ., Stillwater, 1968.
7. Shelton, J., Reid, K. N., “Lateral Dynamics of a Real Moving Web,” ASME Journal Dynamics, Syst. Measurement Control, Vol. 93, 1971, pp. 180-186.
8. Shelton, J., “The Effect of Camber on Handling,” Proceedings of the International Conference on Web Handling, Oklahoma State Univ., Stillwater, 1997, pp. 248-263.

Auto Taper Tension Profile Maker in a Converting Machine

C. W. Lee[1], J. W. Lee[1] & K. H. Shin[1], & S. O. Kwon[2], [1]Konkuk University and [2]Sung-An Machinery, KOREA

Name & Affiliation	**Question**
Tim Walker, TJ Walker & Associates	The models that you employing here for the lateral displacement are models I've seen typically applied for spans between rollers. Are you implying here that the lateral motion in the free span prior to the winder is responsible for the telescoping or are you applying these models to layers inside the roll that are able to slip laterally? Is your telescoping happening as the web approaches the roll or is it winding straight and then shifting inside the roll?
Name & Affiliation	**Answer**
K.H. Shin, Konkuk University	This lateral motion occurs because of the uneven tension distribution across the web just before the winding. So the telescoping we are studying occurs as the web approaches the winding roll.
Name & Affiliation	**Question**
Unknown	If the tension in the web entering the winding roll is varying across the roll width should not the circumferential stress in the outer layer of the roll also vary across the width? In your presentation, you just used average stress. If you use a heaviside function to adjust the winding tension, you introduce a step change in the winding tension. A step in the winding tension would result in a spike in the circumferential tension at the wound roll radius that coincided in time with the step. The winding tension profile like the one shown in Figure 14d will produce a continuous function in radial pressure but the circumferential stress profile would have a very high spike at the roll radius where the step in winding tension occurred.
Name & Affiliation	**Answer**
K.H. Shin, Konkuk University	We tried to smooth out the curve, rather than using the rate of change to reduce the spike. We changed the alpha parameter gradually to minimize the spike.